an energy dependence of the form $1+bW^{-1}$ with an average value of $b=0.17$ has also been reported.[20,25–27] Although this energy dependence is not in serious disagreement with the present measurement, it cannot be reconciled with a recent measurement of the longitudinal β polarization $P=(1.00\pm0.01)v/c$.[28] Analyzing their results of the β-polarization measurement, Wenninger *et al.*[28] concluded an upper limit of 0.008 ±0.025 for the coefficient b. If, however, the shape factor is of the form $C=1-aW$, the β-polarization coefficient is not expected[29,30] to deviate from unity.

[25] R. L. Graham, J. S. Geiger, and T. A. Eastwood, Can. J. Phys. **36**, 1084 (1958).
[26] O. E. Johnson, R. G. Johnson, and L. M. Langer, Phys. Rev. **112**, 2004 (1958).
[27] L. S. Novikov and Ch'ing Ch'eng-Jui, Zh. Eksperim. i Teor. Fiz. **42**, 364 (1962) [English transl.: Soviet Phys.—JETP **15**, 252 (1962)].
[28] H. Wenninger, J. Stiewe, H. Muusz, and H. Leutz, Nucl. Phys. **A96**, 177 (1967).

ACKNOWLEDGMENTS

The author wishes to express his appreciation to Dr. M. S. Freedman for bringing the Ca^{47} problem to his attention and for making his stay at Argonne National Laboratory possible. Thanks are due to Dr. Engelkemeir, Dr. Glendenin, and Dr. Unik for letting the author use various pieces of their apparatus. It is a pleasure to acknowledge the help of Dr. F. T. Porter, P. Day, and F. Wagner. The author is grateful to J. Lerner for performing the Ca^{47} isotope separation.

[29] G. Schatz, H. Rebel, and W. Buhring, Z. Physik **177**, 495 (1964).
[30] B. Eman and D. Tadić, Glasnik Mat.-Fiz. Astron. **1–2** (1961).

PHYSICAL REVIEW VOLUME 173, NUMBER 4 20 SEPTEMBER 1968

Precise Muonic $K\alpha$ Isotope Shifts for Nuclides from Si to Sn†*

R. D. EHRLICH
The Enrico Fermi Institute and Department of Physics, The University of Chicago, Chicago, Illinois
(Received 8 April 1968)

Measurements of muonic $K\alpha$ isotope shifts for 29 nuclides are described in detail. In most cases, these measurements provide unique information on changes in the nuclear charge distribution. The model dependence of the changes in rms radii derived from the muonic shifts (necessary for comparison with electronic data) is discussed in detail. The muonic shifts in Sr, Zr, and Sn are compared with the relevant electronic measurements; the Ca isotope shifts are compared with the results of recent electron scattering results. Strong shell effects are confirmed at $N=28$ and 88, viz., Ca^{48} and Sr^{88} are found to have smaller rms charge radii than Ca^{40} and Sr^{86}. Precise values are also obtained for the K-Ca isotone shifts and for the absolute energies of nine $K\alpha$ transitions.

I. INTRODUCTION

NUCLEAR sizes and shapes, perhaps the most direct manifestation of wave functions of nucleons in matter, are of obvious significance to the understanding of nuclear structure. The measurement of volume-dependent isotope (or isotone) effects can provide a "differential" view of nuclear size which should prove useful both to the study of nuclear systematics and to theories of nuclear matter.

Until several years ago, the study of changes in nuclear size between neighboring nuclides was almost solely the domain of optical spectroscopy. The work on optical isotope shifts (IS), generally restricted to elements with $Z\gtrsim40$, has been extensively reviewed,[1–4] from both its experimental and theoretical aspects. As has been noted elsewhere,[4–7] optical IS often suffer from certain difficulties of measurement and interpretation which are absent in the corresponding muonic cases, viz., the following:

(1) IS for $Z\lesssim50$ are usually comparable to, or much smaller than, the Doppler-shifted linewidth of typical optical transitions;

(2) In many cases, notably Sn [8] and Ru,[9] the so-called specific mass shifts (see Sec. IV), are *a priori* unknown in sign and magnitude, and may well be comparable to the volume shifts in which one is interested.

(3) The complicated electronic configurations involved in typical optical transitions often make it difficult to translate the measured shifts into changes in

* Research supported by the Office of Naval Research and National Science Foundation Grant Gp 6135 (Research).
† A thesis submitted to the Department of Physics, The University of Chicago, in partial fulfillment of the requirements for the Ph.D. degree.
[1] P. Brix and H. Kopfermann, Rev. Mod. Phys. **30**, 517 (1958).
[2] G. Breit, Rev. Mod. Phys. **30**, 507 (1958).
[3] H. Kopfermann, *Nuclear Moments* (Academic Press Inc., New York, 1958).
[4] D. N. Stacey, Rept. Progr. Phys. **29**, 171 (1966).
[5] C. Nissim-Sabat, (Thesis) Nevis Report 129, 1965 (unpublished).
[6] R. J. Powers, Phys. Rev. **169**, 1 (1968).
[7] R. D. Ehrlich, D. Fryberger, D. A. Jensen, C. Nissim-Sabat, R. J. Powers, V. L. Telegdi, and C. K. Hargrove, Phys. Rev. Letters **18**, 959 (1967); **19**, 334 (E) (1967).
[8] D. N. Stacey, Proc. Roy. Soc. (London) **A280**, 459 (1964).
[9] W. H. King, Proc. Roy. Soc. (London) **A280**, 430 (1964).

mean-squared radius, $\delta\langle r^2\rangle$. Uncertainties in calculating the effects of screening of nontransition s electrons by the valence electron, and in estimating $|\psi(0)|^2$ for the valence electron, may limit estimates of $\delta\langle r^2\rangle$ (or, equivalently, βC_{exp}) to $\pm 20\%$.[1-4]

The earliest studies of muonic IS [10,11] used NaI(Tl) as a detector. The marginal resolving power of NaI places severe demands on the stability of experimental system, and results are inevitably dominated by systematic rather than statistical errors. As a consequence, the development of the Ge(Li) detector has greatly advanced the determination of muonic IS.[7,12-16] The large enhancement in resolving power relative to NaI ($\sim$a factor of 20) more than compensates for the poorer detection efficiency. The experimental shifts are generally quite evident to the unaided eye; even crude methods of analysis provide results accurate enough to be compared fruitfully to both the theoretical predictions and other experiments (see, e.g., Fig. 1). Two other methods of studying isotopic changes in nuclear size have also recently become practicable. The work on the Ca isotopes[17-20] and Ti isotopes[21] has demonstrated the power of elastic electron scattering to detect such isotopic variations, thus realizing the promise of a very early study of the Fe and Ni isotopes.[22] Another valuable technique for $Z \gtrsim 40$ is the measurement of electronic K-x-ray shifts with curved-crystal spectrometers. Such shifts have been reported for isotopes of Sn, W, Pb, and U by a Caltech group,[23,24] and for Mo, Nd, and Sm by Sumbaev *et al.*[25,26]

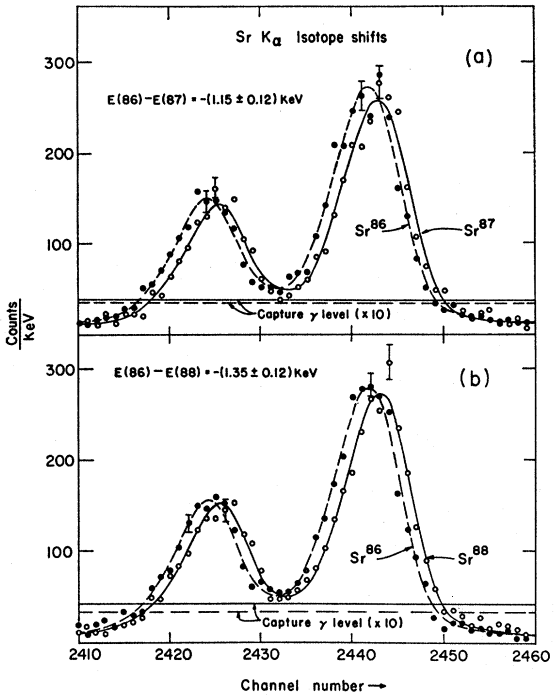

FIG. 1. (a) Muonic $K\alpha$ x-ray spectra for Sr^{86} and Sr^{87} (gain 1 keV/channel). The curves drawn through the data points are best fit to a numerical line shape derived from all Sr^{86} data. For 49 degrees of freedom, one finds $\chi^2(Sr^{86})=47.5$, $\chi^2(Sr^{87})=66.0$. (b) Analogous spectra for Sr^{86} and Sr^{88}; here χ^2 $(Sr^{86})=54.0$, $\chi^2(Sr^{88})=51.1$. Also indicated ($\times 10$) are the capture γ-ray backgrounds, which were subtracted prior to fitting. The fine-structure splitting of $\sim$17.4 keV is clearly resolved.

All the above-mentioned techniques have their own peculiar advantages and limitations. The first goal of this work is to exploit the capability of muonic x rays to precisely measure IS for many nuclides which had not been heretofore studied, and which are inaccessible to optical and electronic x-ray measurements. For these cases, the present measurements provide unique estimates of isotopic changes in charge radius, albeit with possible difficulties of interpretation. Our second aim is to compare, for Ca, Sr, Zr, and Sn, the precise muonic IS with measurements by other techniques. Such comparisons may, on the one hand, provide information about changes of nuclear shape and on the other check the validity of the usual assumptions underlying the interpretation of muonic IS.

Sections II and III treat, respectively, the experimental technique employed, and the method by which the IS are extracted from the data. In Sec. IV we discuss the potential difficulties involved in relating the observed IS to changes in nuclear size. The precision of the present measurements dictates, in particular, re-

[10] J. A. Bjorkland, S. Raboy, C. C. Trail, R. D. Ehrlich, and R. J. Powers, Phys. Rev. **136**, B341 (1964).
[11] R. C. Cohen, S. Devons, A. D. Kanaris, and C. Nissim-Sabat, Phys. Letters **11**, 70 (1964).
[12] C. Chasman, R. A. Ristinen, R. C. Cohen, S. Devons, and C. Nissim-Sabat, Phys. Rev. Letters **14**, 181 (1965).
[13] R. D. Ehrlich, D. Fryberger, D. A. Jensen, C. Nissim-Sabat, R. J. Powers, B. A. Sherwood, and V. L. Telegdi, Phys. Letters **23**, 468 (1966).
[14] H. L. Anderson, R. J. McKee, C. K. Hargrove, and E. P. Hincks, Phys. Rev. Letters **16**, 425 (1966).
[15] H. Daniel, G. Poelz, H. Schmitt, G. Backenstoss, H. Koch, and S. Charalambus, Z. Physik **205**, 472 (1967).
[16] E. Macagno, R. Barrett, S. Bernow, S. Devons, I. Duerdoth, J. Kast, J. Rainwater, K. Runge, and C. S. Wu, Bull. Am. Phys. Soc. **12**, 75 (1967).
[17] R. Hofstadter, G. K. Nöldeke, K. J. van Oostrum, L. R. Suelzle, M. R. Yearian, B. C. Clark, R. Herman, and D. G. Ravenshall, Phys. Rev. Letters **15**, 758 (1965).
[18] K. J. van Oostrum, R. Hofstadter, G. K. Nöldeke, M. R. Yearian, B. C. Clark, R. Herman, and D. G. Ravenhall, Phys. Rev. Letters **16**, 528 (1966).
[19] J. B. Bellicard, P. Bounin, R. T. Frosch, R. Hofstadter, J. S. McCarthy, B. C. Clark, R. Herman, and D. G. Ravenhall, Phys. Rev. Letters **19**, 527 (1967).
[20] K. J. van Oostrum, R. Hofstadter, G. K. Nöldeke, M. R. Yearian, B. C. Clark, R. Herman and D. G. Ravenhall, Bull. Am. Phys. Soc. **11**, 351 (1966).
[21] H. Theissen, R. Engfer, and G. J. C. van Niftrik, Phys. Letters **22**, 623 (1966).
[22] B. Hahn, R. Hofstadter and D. G. Ravenhall, Phys. Rev. **105**, 1353 (1957).
[23] R. T. Brockmeier, F. Boehm, and E. N. Hatch, Phys. Rev. Letters **15**, 132 (1965).
[24] R. B. Chesler, F. Boehm, and R. T. Brockmeier, Phys. Rev. Letters **18**, 953 (1967).
[25] O. I. Sumbaev and A. F. Mezentsev, Zh. Eksperim. i Teor. Fiz. **49**, 459 (1965) [English transl.: Soviet Phys.—JETP **22**, 323 (1966)].
[26] O. I. Sumbaev, E. V. Petrovich, V. S. Zikov, A. S. Ril'nilov, and A. G. Grushko, Yadern. Fiz. **5**, 544 (1967) [English transl.: Soviet J. Nucl. Phys. **5**, 387 (1967)].

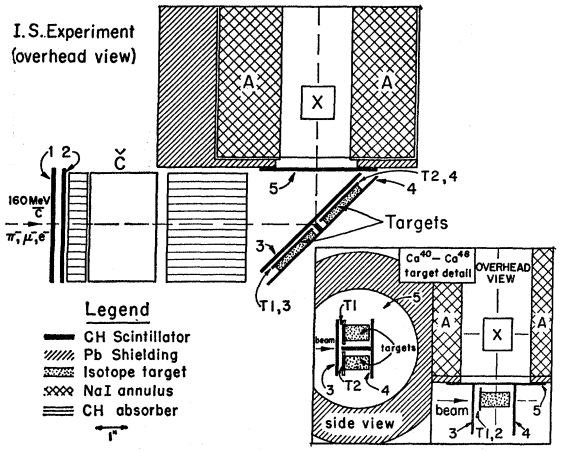

FIG. 2. Arrangement of the muon telescope and the x-ray detector. The insert shows the special target assembly used for the Ca^{40}–Ca^{48} runs. Counter light pipes are not indicated.

consideration of the usual assumption that muonic IS are model-independently proportional to $\delta\langle r^2\rangle$. In Secs. V and VI we present the results for Ca, Sr, Zr, and Sn and their comparison to electron scattering and optical measurements. Section VII surveys the results for all other nuclei studied. Sections VIII and IX cover certain ancillary results, viz., the Ca-K isotone shifts and a set of absolute $K\alpha$ energy measurements.

II. EXPERIMENTAL TECHNIQUE

A. Apparatus

The experiment was performed using apparatus built by collaborative effort of a Canadian group and Anderson's group at this Institute. This apparatus, which will be described in detail elsewhere,[27] closely resembles in its logical functions that used in an earlier Chicago experiment.[6] Enhanced data-collection capability, faster electronics, improved stability, lower backgrounds, and increased automation constitute the main advances of the new system.

1. Muon Telescope

The counter telescope (see Fig. 2) which identifies a muon stop in a particular target was essentially of conventional design. A stopping muon is defined by the signature $123(T_i)\bar{C}\bar{4}\bar{5}$, where the Čerenkov counter $\check{C}$ (filled with FC-75) serves to suppress the electron contamination (~30%) in the 155-MeV/c beam. Muons are separated from pions by range; all pions stop far upstream of the targets. The four counters T_i permit the simultaneous study of an equal number of distinct targets. "Cross-talk" produced by muons scattering from one target into another is essentially eliminated by the peculiar shape of counter 4: This has a cross-shaped scintillator rib separating the targets.

Typically, the muon stop rate over all four targets was 1.3×10^4/sec g cm^{-2}. For the actual targets used (except for Ca^{48}, see below) this corresponds to stop rates of from 1.5×10^3/sec to 4.0×10^3/sec per target. The targets were either metals or pure compounds, cast or pressed into 5×5-cm squares, and enclosed in thin Lucite boxes. Because of the very small amount of Ca^{48} available, a special counter-target arrangement was employed for the Ca^{40}–Ca^{48} runs (see insert to Fig. 2). Here only two small target counters, placed one above the other, and as close to the detector as practicable, were used. These targets consisted of ~4.0 g of CaO pressed into Al pill boxes ($\frac{1}{2}$ in. in diameter, 1 in. long, and with 0.010-in.-thick walls). About 150 muons/sec were stopped in each target.

2. γ-Ray Detection System

The γ-ray detector X was a 17-cm^3 coaxial Ge(Li) diode.[28] It was surrounded by an annulus of NaI, A, which could be brought into anticoincidence with pulses in X. The signature $X(\bar{A})$ was used for γ rays below about 3 MeV; here it effectively suppresses Compton interactions, thus enhancing the peak-to-background ratios. Above 3 MeV, where pair production dominates, the information from the annulus was ignored.

The amplification system consisted of a cooled FET preamplifier, and a main amplifier (Tennelec TC-200) followed by a linear gate. The analog-to-digital converter (ADC, Nuclear Data model 181), had 4096 channels, digitally stabilized against both gain changes and zero shifts. Data were taken at a nomial gain of 1.0 keV/channel for targets with $Z\geq38$ and at twice the gain for the others. Two precision mercury pulsers provided references for the digital stabilizer; a third pulser was periodically stepped over the entire range of the ADC, providing an on-line monitor of system response. All components were maintained in an air-conditioned environment.

3. Event Labeling and Storage

The fast logic identified six basic kinds of event: (1) γ rays associated with a muon-stop in any of four specific targets; (2) a calibration pulse in anticoincidence with the beam; (3) a source γ ray, in anticoincidence with the beam and the pulser. Each type of event set an appropriate tag bit in an interface register communicating with a computer (PDP-8). As a precaution against rate-dependent effects, all events were gated so as to be accepted only during the beam spill time. An electronic time-interval meter (Eldorado Electronics) was started by a muon-stop pulse, and stopped by the associated pulse in the Ge detector. The muon-associated events

[27] H. L. Anderson, R. J. McKee, R. Barton, F. Castorf, C. K. Hargrove, E. P. Hincks, and J. McAndrew (to be published).

[28] Kindly lent us by Atomic Energy of Canada, Ltd., Chalk River Nuclear Laboratories.

were thus classified as (a) prompt x rays, or (b) delayed-capture γ rays, in accordance with the measured time interval. Hence the muon-capture γ-ray backgrounds were stored concurrently with the muonic x rays. The tag sorting and some storage were performed by the PDP-8 computer; the bulk of the spectra were stored in an ASI 6040 computer. Almost 24 000 12-bit words or "channels" were used for spectrum storage.

The system briefly described above constitutes a powerful tool for most muonic x-ray experiments. It possesses, however, features which were especially valuable for isotope shift studies; these we shall discuss at greater length below.

B. Application to IS Measurements

This experiment was designed with three goals in view: (a) measurement of the IS to high statistical precision with minimal error from anticipated systematics; (b) ability to check the most prominent sources of anticipated systematic error; and (c) efficient use of accelerator time and of the avialable separated isotopes.

High statistical precision was to be attained, not merely by collecting large amounts of data, but by ensuring that the linewidths were narrow and backgrounds small, and that isotope-dependent backgrounds were well determined. The clean geometry, veto annulus, high instrumental stability, and simultaneous measurement of delayed γ-ray backgrounds were of advantage in this respect.

The use of multiple targets was central to the attainment of all three goals. Most obvious is the relation to point (c). Since we had in no case sufficient quantities of isotopes to stop more than a fraction of the beam, our data accumulation rate was enhanced almost fourfold by the use of four targets. More important, though, are the advantages which accrue from nearly total elimination of systematic errors. These are: (1) time- and/or rate-dependent instrumental drifts or distortions which may give rise to spurious IS; (2) possible asymmetries related to differing target-detector geometries; (3) possible shifts arising from different source thicknesses. The first two sources of error are closely interrelated. Simultaneous accumulation of the x rays ensured, for a given target configuration, that the IS were insensitive to drifts and rate effects. The use of multiple targets, however, necessitates precaution against position dependent errors (point 2, above). The effect of potential positional asymmetries was minimized by periodically permuting the various targets belonging to a given set, so that the total accumulated spectra for each isotope were good averages over all four positions. The averaged IS should then be entirely free from spurious shifts due to (1) and (2). In most cases, each isotope was matched to a comparison target of equal thickness; for these, errors due to (3) vanish. When the target thicknesses were not matched, the apparent IS could be biased at most by the Compton energy loss suffered in traversing ≈ 1 g/cm^2 of material. This we estimate to be ≤ 0.05 keV.

Elimination of systematic errors did not merely depend on the careful application of the procedure outlined above. It was possible to monitor drifts and to perform several null experiments which further reinforce our confidence on the results. Approximately every 20 min, during the course of data collection, the precision pulser was stepped through 20 voltages covering the entire range of the ADC. For each step, the main computer (ASI) stored the applied pulser voltages and the centroids of the resulting pulse-height distributions. After completion of each cycle, it fitted a polynomial to the centroids as a function of pulser voltage. The conversion factor between pulser voltage and γ-ray energy being known, changes in the parameters of this fit could be readily related to the drifts in nominal x-ray energies. The estimated drift between successive 6- to 8-h runs was typically less than 0.1 channel (0.1 keV or less), and in no case were corrections for drifts necessary. Although potential geometrical asymmetries were eliminated by target permutation, several tests showed them to be in fact absent. The Ca^{40}–Ca^{42} and Ca^{40}–Ca^{44} isotope shift runs were performed with two targets of each isotope, while a high-statistics run had Ca^{40} metal in all four positions. Analysis showed all like targets to yield within statistical error (± 0.04 keV) the same x-ray energy.

Differential nonlinearity (local fluctuation in channel width) was checked, before the experiment, by a sliding pulser technique and was found to be negligibly small ($<10\%$). The extremely good integral linearity ($<0.1\%$) was especially useful in the absolute energy measurements as was the simultaneous accumulation of source γ-ray spectra.

III. DATA ANALYSIS

After each isotope run with the targets in a given permutation, the spectra stored in the two computers were dumped onto magnetic tape, along with other information pertinent to the run. The tapes were processed and printouts of all spectra examined. The prompt muonic x-ray spectra were then corrected for the contribution from capture γ rays, by subtracting from them an appropriate fraction of the concurrently accumulated delayed spectra. This fraction is fixed by the time resolution of the Ge(Li) detector and the relevant muon capture lifetime. Capture lifetimes were taken, where possible, from experimental data; where no data existed, the Primakoff formula[29] was used for interpolation. In no case did the delayed spectra show structure in the region of interest, and therefore the subtractions hardly affected the data (or the IS results). For the Sr^{86} and Sr^{88} targets, for example, the capture corrections amounted to removing background levels of 3.2 and 4.4 counts/channel, respectively. The cor-

[29] H. Primakoff, Rev. Mod. Phys. 31, 802 (1959).

TABLE I. Composition of isotopic samples.

Sample	Mass of isotope (g)	Chemical form	Composition (%)					
			Si^{28}	Si^{29}	Si^{30}			
Si^{28}	···	SiO_2	92.3	4.7	3.1			
Si^{29}	39	SiO_2	4.3	95.3	0.4			
Si^{30}	40	SiO_2	3.8	0.6	95.6			
			K^{39}	K^{41}				
K^{39}	59	KCl	93.1	6.9				
K^{41}	59	KCl	0.9	99.1				
			Ca^{40}	Ca^{42}	Ca^{44}	Ca^{48}		
Ca^{40}	···	CaO	96.9	0.6	2.1	0.2		
Ca^{42}	95	CaO	5.3	93.8	0.8			
Ca^{44}	189	CaO	1.4		98.5			
Ca^{48}	2.4	CaO	2.8		0.1	97.1		
			Fe^{54}	Fe^{56}	Fe^{57}	Fe^{58}		
Fe^{54}	100	Metal	97.1	2.9				
Fe^{56}	···	Metal	5.9	91.5	2.2	0.3		
Fe^{57}	27	Fe_2O_3	0.1	9.0	90.7	0.2		
			Ni^{58}	Ni^{60}	Ni^{61}	Ni^{62}		
Ni^{58}	100	Metal	99.9	0.1	0.0	0.0		
Ni^{60}	200	Metal	0.2	99.8	0.0	0.0		
Ni^{61}	44	Metal	1.8	5.2	91.9	1.0		
Ni^{62}	50	Metal	0.5	0.8	0.0	98.7		
			Cu^{63}	Cu^{65}				
Cu^{63}	81	Metal	99.9	0.3				
Cu^{65}	94	Metal	0.3	99.7				
			Sr^{84}	Sr^{86}	Sr^{87}	Sr^{88}		
Sr^{86}	142	SrF_2	0.0	97.0	0.9	2.1		
Sr^{87}	114	SrF_2						
Sr^{88}	···	SrF_2	0.6	9.8	7.0	82.7		
			Zr^{90}	Zr^{91}	Zr^{92}	Zr^{94}	Zr^{96}	
Zr^{90}	150	ZrO_2	97.7	1.0	0.7	0.6	0.1	
Zr^{92}	41	ZrO_2	2.3	0.9	95.7	1.0	0.1	
			Sn^{116}	Sn^{117}	Sn^{118}	Sn^{119}	Sn^{120}	Sn^{122}
Sn^{116}	90	Metal	95.8	1.0	1.5	0.3	1.1	0.3
Sn^{117}	34	Metal	2.6	89.2	4.5	1.1	2.2	0.6
Sn^{118}	84	Metal	0.4	0.4	97.2	0.6	1.2	0.3
Sn^{119}	70	Metal	0.7	0.6	3.0	9.8	5.3	0.6
Sn^{120}	154	Metal	0.3	0.0	0.5	0.4	98.4	0.4
Sn^{122}	41	Metal	1.0	0.6	1.9	0.8	3.8	92.0

responding $K\alpha_1$ peak channels contained ~300 counts (see Fig. 1).

The corrected spectra may be analyzed for the IS in several ways. One approach[5] is to subtract a structureless backgound from the data and to then calculate the centroid of the residual x-ray peak. The difference between centroids for two isotopes is presumed to correspond uniquely to the true IS. This method suffers from several difficulties which outweigh the virtue of its simplicity. The centroids are calculated over a finite range of channels; the choice of this range frequently tends to bias the final result, unless the range is very large compared to the peak width. In the latter case however, the deduced centroid becomes very sensitive to the assumed background, and the method loses statistical power.

A second approach often used[13] is to fit the experimental data by a multiparameter analytic form for the peak and background. With $K\alpha$ fine structure (FS) unresolved (or barely resolved) and asymmetric line shapes, as many as ten or more parameters may be needed for a good fit. The principal disadvantage is statistical. The only parameter of relevance is the "peak position," whose change gives the IS. By fitting the other spectral shape parameters one pays the price of reduced statistical power in determination of the "peak position." This technique was used by us primarily to check the results obtained by a third method outlined below.

All the IS reported here were derived in a manner similar to the analytic multiparameter fit, but by a method which is simpler and more powerful. This method[30] exploits the similarity of spectra from different isotopes. It consists in replacing the *analytic* line shape by an interpolated, *numerical* line shape derived from the muonic x-ray data from an abundant isotope. Specifically, we subjected the corrected x-ray spectrum from this "reference" target to a parabolic smoothing routine, and then interpolated it at intervals of 0.05 channels by a four-point Lagrangian interpolation formula. The resulting numerical function is the "master line shape." An analysis program shifted the individual isotope spectra relative to the properly normalized master line shape by successive steps of 0.05 channels. The channel shift which optimized a suitable criterion of goodness-of-fit determined the "position" of a given x-ray line, and the difference in the "positions" of two isotopes, the IS. Goodness-of-fit was measured by both the conventional χ^2 and by a likelihood measure, the latter taking into account the Poisson statistics of the data. Both measures agreed within their respective accuracies, but the likelihood method gave more consistent results for the low statistics runs. We assigned as one statistical standard deviation in peak position that change which induced an increase in χ^2 by unity and decreased the natural logarithm of the likelihood function by one-half. In all cases where the χ^2 for the fit to an x-ray line was greater than the statistical expectation, the associated error in position was increased by the factor $(\chi^2/\chi^2_{\text{exp}})^{1/2}$.

The smoothed master line shapes gave generally good fits to the data, and showed only a weak correlation to the raw data from which they were derived, in the sense that they fitted those data with the statistically expected χ^2. The method was checked in several ways; other techniques gave results in agreement, but with larger errors. Most isotope pairs were analyzed both run by run, and after summing over all target permutations. No significant disagreement was found among the various determinations of a given IS. Likewise, several isotope pairs were analyzed with and without correction for capture γ's. The resulting IS never differed significantly. The only correction applied to the measured IS consisted in allowing for the isotopic impurities of the targets. Because of the high purity (see Table I) of most of these, this correction was usually quite small compared to the statistical errors. It was assumed that the measured peak position of a line from an "impure" target corresponds to the weighted mean of the positions of its isotopic constituents. The corrected IS could then be derived from the measured shifts and the known

[30] I am grateful to Professor V. L. Telegdi for suggesting this approach.

isotopic compositions by solving a set of simultaneous equations. The conversion of an IS measured in channels to an energy difference entails knowing the gain of the linear system only near the transition energy, and that only to moderate accuracy. The excellent linearity and stability of the system used made this conversion trivial. The nominal gain was 0.50 keV/channel for most isotopes and 1.00 keV/channel for Sr, Zr, and Sn. The calibration was obtained with γ-ray sources in conjunction with the precision pulser.

A byproduct of this experiment was the determination of the absolute muonic $K\alpha$ energies for the elements involved. Here Lorentzian line shapes (with a linear background) were fitted to the lines provided by the calibration sources. The x-ray peaks were (except in the case of Sn where the FS is very clearly resolved) similarly located, except that two Lorentzians with fixed separation and fixed relative widths and peak heights (2:1) were fitted to the data. Inasmuch as it is not certain that the FS components are in practice in the assumed theoretical ratio,[13] the errors in the quoted center of gravity have been adjusted to allow for a 25% uncertainty in that ratio. In Sn the $2p_{3/2}-2p_{1/2}$ FS separation is well resolved and could be accurately measured by the methods empolyed for the IS analysis. The absolute energies (Table VIII) were corrected for isotopic impurities; these corrections were not entirely insignificant at our level of accuracy.

The gain curve (keV versus channel number) was obtained by fitting a three- or four-term polynomial to the four source peak energies. The importance of nonlinear terms was minor (the integral linearity being better than 0.1%), and this calibration introduced significant uncertainties only in the cases of Ne^{60} and Si^{28}, where an extrapolation of the response was necessary. In all cases we used as a guide the on-line precision pulser data, which indicated that the system response could be well fitted over all 4096 channels by an expression of the form

$$E(C)=A_0+A_{-1}/C+A_1C+A_2C^2$$

(where E= energy, C= channel number). The simplicity of the over-all response assured us of the absence of pathologies in the energy regions including the x rays and calibration sources.

IV. INTERPRETATION OF ISOTOPE SHIFTS

The energy levels of a muonic atom may be shifted from those predicted for an infinitely massive pointlike nucleus by three effects, viz., nuclear recoil, finite charge distribution, and nuclear polarization (dispersion shift).

Nuclear recoil results in the so-called reduced mass correction, which is trivially calculable and hence need not be discussed. The shift due to finite nuclear extent, of primary interest to us, is in principle calculable to arbitrary accuracy for a given charge distribution.

The third effect, however, arising from virtual excitation of nuclear states by the muon, depends on details of nuclear structure, and cannot be calculated accurately. However, except for the case of strongly deformed nuclei where the electric quadrupole field of the muon charge distribution may actually excite low-lying rotational states,[31,32] "giant resonances" are expected to contribute most to the level shifts. Pieper and Greiner[33] and Cole[34] have most recently estimated the $1s$ and $2p$ dispersion shifts. Both calculations, although their acutal predictions are not in close agreement, show the contribution ($\sim$0.5 keV for the Sn $K\alpha$ transitions) of the giant $E1$ resonance to predominate.

Specifically relevant to the problem of muonic IS is, of course, the variation of the dispersion shifts from one isotope to another. Assumption of an $A^{-1/3}$ dependence for the energy of the giant resonances yields the result that the dispersion corrections to the muonic $1s$ and $2p$ levels in neighboring Sn isotopes differ at most by few eV. Granting this assumption, we shall ignore dispersion effects in our interpretation.

Ideally, muonic IS would be used to check predicted or measured nuclear charge distributions. Given an explicit charge distribution for each member of an isotopic pair, one readily obtains by numerical integration the relativistic energy eigenvalues in the corresponding electrostatic potential (as modified by vacuum polarization). The energy differences (e.g., for the $K\alpha$ transitions), may be directly compared with the experimental shifts. This procedure was, in fact, followed for the Ca isotopes, for which phenomenological charge distributions based on elastic electron scattering[17–20] experiments exist. For most nuclei, however, no such detailed information is available. Here one attempts to extract from the IS corresponding changes in a moment of the charge distribution. Traditionally, IS are expressed as $\delta(R_u)/\delta(R_u)_{\rm std}$, where $R_u^2=(5/3)\langle r^2\rangle$, and $\delta(R_u)=R_u(A_2)-R_u(A_1)$, $\delta(R_u)_{\rm std}/R_u=A_2^{1/3}-A_1^{1/3}\simeq\frac{1}{3}\delta A/A$. Electronic IS, to the extent that they may at all be related unambiguously to changes in nuclear size, are closely and model-independently proportional to $\delta(R_u^2)$. Muonic IS on the other hand, because of their much greater sensitivity to details of the nuclear charge distribution, may be expected to depart from a strict linear dependence on R_u^2. As an example, consider the case of Ca. Here quite different models which predict the same absolute $K\alpha$ energy of say, Ca^{40}, yield the same value of R_u to better than 0.7%. Nevertheless the smallness of $\delta(R_u)_{\rm std}/R_u$ ($\sim$0.02) suggests that the model dependence of $\delta(R_u)$ is even for such relatively low-Z nuclides a non-negligible source of uncertainty. It can be particularly significant for the present results whose *statistical* precision is sufficient to determine

[31] R. D. Ehrlich, R. J. Powers, V. L. Telegdi, J. A. Bjorkland, S. Raboy, and C. C. Trail, Phys. Rev. Letters **13**, 550 (1964).
[32] S. A. DeWit, G. Backenstoss, C. Daum, J. C. Sens, and H. L. Acker, Nucl. Phys. **87**, 657 (1967).
[33] W. Pieper and W. Greiner, Phys. Letters **24B**, 377 (1967).
[34] R. Cole, Jr., Phys. Letters **25B**, 178 (1957).

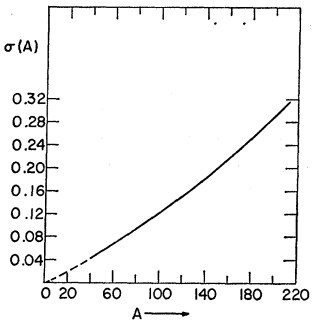

FIG. 3. Plot of the model-dependent uncertainty $\sigma(A)$ in $\delta(R_u)/\delta(R_u)_{\rm std}$ versus A for $|\delta t/t|=0.05$ and $\Delta A=2$.

$\delta(R_u)/\delta(R_u)_{\rm std}$ in favorable cases, such as Sn, with an uncertainty of only ± 0.03.

We shall now explore the model dependence of $\delta(R_u)$ within the framework of a particular phenomenological charge distribution, viz., the Fermi shape[25]

$$\rho_F(r)=N(c,s)/[1+\exp((r-c)/s)], \quad (1)$$

where c is the half-density radius, $t=s(4\ln 3)$ is the skin thickness, and $N(c,s)$ is the normalization factor. For this charge distribution, one has, to an excellent approximation,

$$R_u^2=c^2+1.19t^2. \quad (2)$$

If t were a universal constant, there would be no model dependence in the interpretation of muonic IS, and these could be related uniquely to the corresponding electronic shifts. Whereas this is certainly not the case in nature, it has nevertheless been shown by Elton[35] that (1) fits well the electron scattering results and muonic transition energies in the large (i.e., over a wide range of A) with a *constant* t, equal to 2.35 F. We shall assume that this constancy of t holds, at least approximately, in the small (i.e., for IS) as well. We shall term the assumption $\delta t=0$ our "reference model," and denote the corresponding estimates of δR_u as $\delta(R_u)_t$. Clearly,

$$\delta(R_u)_t\equiv\frac{\delta E}{(\partial E/\partial R_u)_t},$$

where E is the $K\alpha$ transition energy. To display deviations from the reference model, we expand E to first order in $\delta(R_u)$ and δt, obtaining

$$\delta(R_u)_t=\delta(R_u)-\delta t(\partial R_u/\partial t)_c(1-K_c/K_t),$$

where

$$K_c=(\partial E/\partial R_u)_c, \quad K_t=(\partial E/\partial R_u)_t.$$

Using (2) and the definition of $(\delta R_u)_{\rm std}$, one has

$$\sigma=\frac{\delta(R_u)-\delta(R_u)_t}{\delta(R_u)_{\rm std}}\simeq 3.57\frac{A}{\delta A}\frac{t^2}{R_u^2}\left(1-\frac{K_c}{K_t}\right)\frac{\delta t}{t}. \quad (3)$$

This quantity represents the model-dependent uncertainty in $\delta(R_u)/\delta(R_u)_{\rm std}$. We have evaluated K_c and K_t for Ca, Sn, and Pb, finding that to a fair approximation $(1-K_c/K_t)=0.01+7.5\times 10^{-4}\,A$. Figure 3 displays $\sigma(A)$ for $\delta A=2$ and $\delta t/t=0.05$. Manifestly, even for $A\sim 40$, σ is comparable to the statistical precision in $\delta(R_u)_t/\delta(R_u)_{\rm std}$, and there is certainly no *a priori* reason to exclude changes in t of the assumed magnitude (5%) between isotopes differeing by two neutrons. In fact, electron scattering[17–20] indicates variations in t of about 10% among the Ca isotopes. Furthermore, in the regions of permanently deformed nuclei, small changes in the mean-squared deformation $\langle\beta^2\rangle$ correspond to substantial changes in the (spherically averaged) nuclear "skin," viz., $\delta t\propto c\delta\langle\beta^2\rangle$.

It is natural to consider the possibility of using the IS in higher transitions (e.g., $3d_{5/2}\rightarrow 2p_{3/2}$, $3d_{3/2}\rightarrow 2p_{3/2}$, $2s_{1/2}\rightarrow 2p_{1/2}$) to determine δt. These should generally show measurable IS and could be analyzed much as were the $K\alpha$ transitions, but with different values for K_t and K_c.

The IS in the $3d$-$2p$ transitions (L x rays) have considerably greater relative sensitivity to δt than the $K\alpha$ lines. The *absolute* L-x-ray IS are however, even for $Z=50$, so small as to require unreasonable (~ 1 eV) accuracies to contribute significantly to the determination of δt. On the other hand, while the $2s$-$2p$ IS are much larger, the yield of these transitions is so small (about 10^{-3}/muon[36]) as to require extremely long running times.

It has been suggested[4,5,13] that muonic IS might be employed to "normalize" those optical results whose interpretation is obscured by the difficulties mentioned in the Introduction. The preceding discussion suggests that such a procedure will in general be of only restricted usefulness in the absence of independent information on changes of shape. On the other hand, the model dependence of $\delta(R_u)$ can be exploited to obtain estimates of isotopic changes in t in those cases where the electronic IS do give accurate values of $\delta(R_u)$.

Model-dependent effects for low-energy electron scattering have been treated by Theissen *et al.*[21] for the Ti isotopes, in a spirit somewhat similar to our "reference model" discussed above.

V. Ca ISOTOPES: RESULTS AND DISCUSSION

We have shown in Sec. IV that, even in the absence of dispersive effects, the muonic IS are not uniquely determined by $\delta(R_u)$. Thus it is not possible to compare electronic and muonic shifts in a completely satisfying way, since the electronic results provide at best values for $\delta(R_u)$. The situation is much different, however, for the calcium isotopes. Here, very precise electron scattering measurements[17–20] provide phenomenological charge distributions, and what is most relevant, well-determined changes in several parameters describing these.

[35] L. R. B. Elton, *Nuclear Sizes* (Oxford University Press, London, 1961).

[36] C. K. Hargrove (private communication).

TABLE II. Ca isotope shifts.

Isotope pair	Observed muonic $K\alpha$ shift (keV)			Electron scattering prediction[a] Ref. 37
	This expt.	Ref. 10	Ref. 11	
40–42	0.69±0.06	···	···	0.82±0.20
40–44	0.89±0.05	0.9±0.3	0.5±0.3	0.61±0.10
40–48	−0.47±0.12	···	···	−0.54±0.08

[a] These predictions differ from those quoted in our Ref. 7 and reflects more refined analyses by the authors of Ref. 18.

It is thus possible to predict the muonic IS with an accuracy comparable to that achieved in the present experiment.

Agreement between the two techniques depends only on (1) electromagnetic equivalence of the muon and electron, and (2) the absence of significant isotope-dependent dispersion corrections. We may hopefully conclude that such an agreement implies the corrections of *both* (1) and (2) and thus that the electron scattering results for the Ca isotopes in fact determine the changes in shape of a static charge distribution.

Table II compares the experimentally observed muonic shifts (Fig. 4) with the predictions derived from electron scattering.[37] The agreement is excellent, except perhaps for the case of Ca^{40}–Ca^{44}. The errors associated with the electron scattering predictions are, however, purely statistical and should be considered as provisional. In particular, a remarkable result of electron scattering, viz., Ca^{48} has a more "compact" charge distribution than Ca^{40}, is confirmed. It is perhaps worthwhile to stress once again that the muonic IS are, even for Ca, strongly model-dependent. If we attributed the ture $\delta(R_u)$ for Ca^{40}–Ca^{48} solely to change δc in half-density radius, we would expect an IS (apart from the reduced mass shift) approximately twice that observed.

The phenomenological charge distribution used to analyze the electron scattering data, a parabolically deformed Fermi function, is only one of a variety of functional forms which provide a good fit to the data, but it has been shown[18] that the predicted muonic IS do not strongly depend on the model used if that model provides a good fit. We may further check the applicability of that distribution by comparing the absolute Ca^{40} $K\alpha$ x-ray energy with that predicted using the parameters given in Ref. 19.

A. Ca^{40} $K\alpha$ Absolute Energy

We find for the absolute energy of the center of gravity of the $K\alpha$ doublet in Ca^{40}, $E(K\alpha)_{\rm exp}=(783.56\pm0.16)$ keV, using the procedure described in Sec. III. This value is in good agreement with the most recent measurements by other groups[38,39] (see Table VII). For

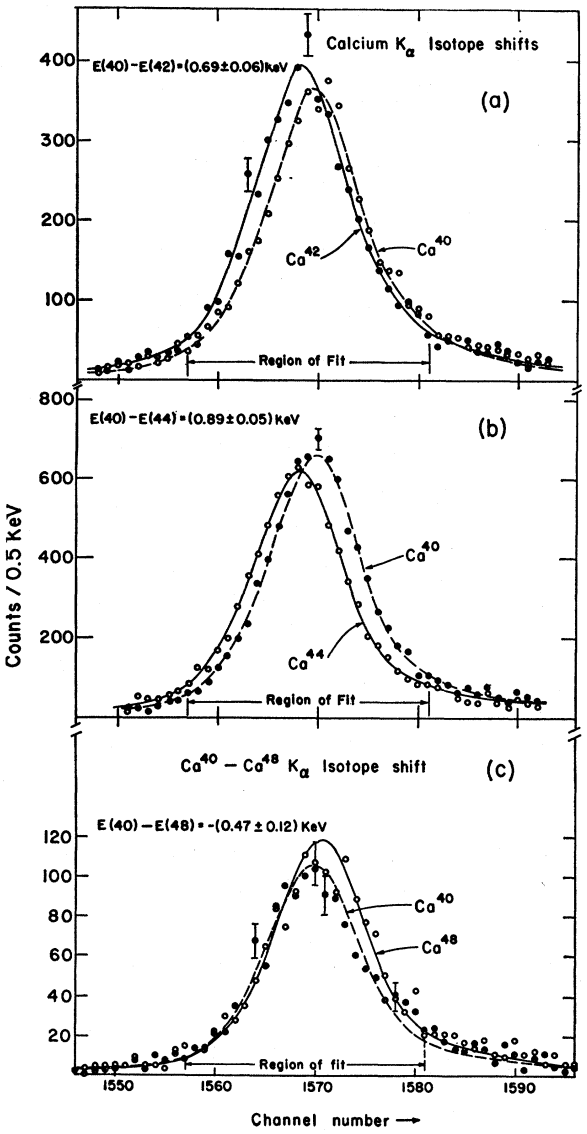

FIG. 4. Muonic $K\alpha$ x-ray spectra for (a) Ca^{40}–Ca^{42}, (b) Ca^{40}–Ca^{44}, and (c) Ca^{40}–Ca^{48} (gain 0.5 keV/channel). The curves drawn through the data points are best fits to a numerical line shape derived from an independent set of Ca^{40} data. For 24 degrees of freedom, one finds (a) $\chi^2(Ca^{40})=15.4$, $\chi^2(Ca^{42})=40.0$, (b) $\chi^2(Ca^{40})=23.5$, $\chi^2(Ca^{44})=17.1$, and (c) $\chi^2(Ca^{40})=29.7$, $\chi^2(Ca^{48})=33.0$.

the distribution:

$$\rho(r)=N(c,s,\omega)(1+\omega^2r^2/c^2)\rho_F(r;cs),$$

with[19] $c=3.6685$ F, $s=0.5839$ F, and $\omega=-0.1017$, we predict $E(K\alpha)_{\rm scatt}=783.64$ keV, including the effects of vacuum polarization. This value is reduced to 782.8 keV upon correction of the nominal 250-MeV beam for target energy loss.[37] Another independent fit[37] to the 250-MeV Ca^{40} data, however, predicts $E(K\alpha)_{\rm scatt}=783.76$ keV. Hence, we may conservatively adopt $E(K\alpha)_{\rm scatt}=(783.3\pm2)$ keV for our comparison. The

[37] D. G. Ravenhall (private communication).
[38] H. L. Acker, G. Backenstoss, C. Daum, J. C. Sens, and S. A. DeWit, Nucl. Phys. **87**, 1 (1966).
[39] A. Suzuki, Phys. Rev. Letters **19**, 1005 (1967).

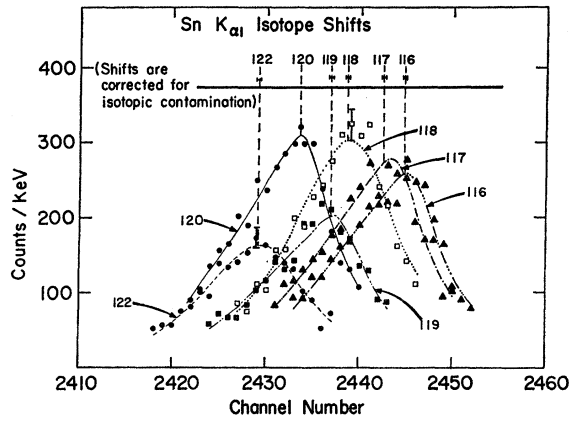

FIG. 5. Sn$K\alpha_1$ spectra (2-quantum escape peaks). Gain: 1.00 keV/channel. These are only a fraction of the data used to establish the IS's. The corrected shifts are also indicated. The curves drawn through the data points are best fits to a numerical line shape derived from all Sn^{120} data.

uncertainty stems largely from model dependence and, to a lesser degree, from experimental uncertainties.

The close agreement on the Ca^{40} $K\alpha$ energy is an independent confirmation of the mutual consistency of the electron scattering and muonic x-ray techniques. If this consistency is taken as established, the very accurately measured x-ray energies may be fruitfully used as additional data (constraints) in electron scattering.[40]

VI. Sn, Sr, AND Zr ISOTOPES: RESULTS AND DISCUSSION

Most of the Sr, Zr, and Sn isotopes for which we present data have been previously studied by optical

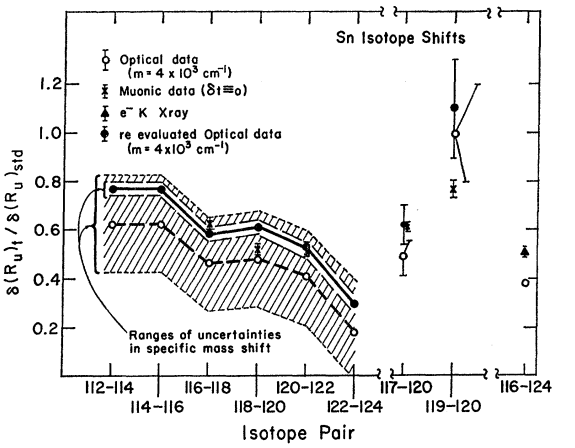

FIG. 6. Brix-Kopfermann plot for the Sn isotopes. Comparison is made to the optical data of Ref. 18 for a specific mass shift of 4×10^{-3} cm^{-1} (heavy dashed line) and with a reevaluated specific mass shift of $(3.0\pm0.4)\times10^{-3}$ cm^{-1} (heavy full line). The shaded and open bands indicate the corresponding bounds on the IS due to the specific mass uncertainty.

[40] Suggested by R. Hofstadter at International Conference on Electromagnetic Sizes of Nuclei, Ottawa.

TABLE III. Sn isotope shifts.

Isotope pair	Observed shift (keV)	Volume shift (keV)	$\delta(R_u)_t/\delta(R_u)_{std}$
116–120	11.55±0.20	11.67	0.558±0.010
117–120	9.28±0.15	9.37	0.620±0.010
118–120	5.17±0.10	5.23	0.521±0.014
119–120	3.42±0.17	3.45	0.768±0.030
120–122	4.95±0.15	5.01	0.508±0.016
116–118	6.38±0.22	6.44	0.630±0.023
118–120	5.17±0.10	5.23	0.521±0.014
120–122	4.95±0.15	5.01	0.508±0.016

techniques. The Sn isotopes are for a number of reasons particularly interesting for a comparison of the IS obtained by very different techniques, viz., the following:

(a) Eight independent optical IS and five independent muonic IS have been measured with high precision;

(b) The Sn^{116}–Sn^{124} shift in *electronic* K x ray has also been determined[24] quite accurately;

(c) The similar nuclear level structures of the even Sn isotopes, and the "stiffness" of these nuclei, suggest that dispersive effects will have little effect on the comparison; and

(d) A determination of the *a priori* unknown *specific* mass shifts afflicting the interpretation of the optical Sn data can be expected to result from the comparison.

Our muonic IS for Sn (see Fig. 5) and the corresponding values of $\delta(R_u)_t/\delta(R_u)_{std}$ are listed in Table III. The same data are also displayed graphically in Fig. 6, in a manner analogous to the Brix-Kopfermann[1] plot traditional in optical spectroscopy. This plot also displays the extensive optical results of Stacey[8] as well as the one *electronic* x-ray IS available, measured by Chesler *et al.*[24]; the optical results are connected (for the even isotopes) by a heavy broken line which serves to indicate the trend of the volume shifts with A. The cross-hatched region whose boundaries follow this line indicates the uncertainty introduced in the interpretation of the optical IS by the only approximate knowledge of the *specific* mass shift m for the relevant optical transition (for details, see below). Note that m (per neutron) is common to all the IS, so that any change in the value of m from that determined by Stacey corresponds to a vertical displacement of the entire heavy broken line in Fig. 6. As discussed in Sec. IV, the interpretation of the observed muonic IS in terms of a change $\delta(R_u)$ is model-dependent, whereas the electronic IS are free from this ambiguity. In preparing Fig. 6, we have adopted our "reference model" for changes in the nuclear charge distribution, i.e., used $\delta(R_u)_t$. The assumption of constant skin thickness t is obviously immaterial for the electronic IS. It may be seen from Fig. 6 that the optical IS as estimated by Stacey are in only fair agreement with both the muonic IS and the electronic $K\alpha$ Sn^{116}–Sn^{124} IS of Ref. 24. In what follows, we shall investigate the probable reasons for these discrepancies.

It is useful to note that, for all three techniques, the observed IS $\delta_\lambda^{NN'}$ between neutron numbers N and N' for a given transition λ may be written as the sum of two terms (after correction for the normal mass effect), i.e., in Stacey's notation[4]

$$\delta_\lambda^{NN'}=F_\lambda C^{NN'}+m_\lambda(N'-N) \quad (4a)$$

or

$$\delta_\lambda^{NN'}=K_\lambda\delta(R_u^2)^{NN'}+m_\lambda(N'-N). \quad (4b)$$

In (4a), $C^{NN'}$ is the optical IS constant and is proportional to $\delta(R_u^2)$. F_λ and K_λ depend only the relevant electronic (muonic) configurations and are, in ordinary atoms, proportional to $|\psi(0)|^2$ for the relevant electron. In this discussion we neglect the model dependence of K_λ in the muonic IS. The specific mass shift m_λ is absent in muonic IS and can be reliably estimated for electronic x-ray shifts.

The structure of Eq. (1) has several important implications, first emphasized by King.[9] If the IS for two or more isotope pairs are measured in two different transitions (electronic or muonic), knowledge of F(or K) in one transition determines F (or K) in the other; knowledge of m_λ in one transition (λ) determines m_λ, in the other (λ'). Since for muonic transitions K is (at least for a specified model) accurately calculable (and $m\equiv 0$), one can, in principle, use the muonic shifts to determine both K and m for the transition (3283 Å) studied in Ref. 8.

In practice, it is more useful to constrain the electronic factor K to a value derived from a comparison of the IS in the 3283-Å transition with the work of Hindmarsh and Kuhn[41] at 6454 Å. $M1$ hyperfine structure (hfs) in the latter transition determines F(6454 Å) and F(3283 Å) to perhaps $\pm 5\%$.[42] This accuracy far exceeds that which could be attained from a comparison of the muonic and optical data, hence we shall choose to adjust only the specific mass shift m for best agreement between the muonic and optical IS. This is equivalent to a vertical transition of the Brix-Kopfermann plot in Fig. 6. The same procedure may be carried out with the optical and electronic x-ray IS between Sn^{116} and Sn^{124}.

Chesler *et al.* express their result as $\delta(\Delta E)_{\text{expt}}/\delta(\Delta E)_{\text{std}}=0.504\pm 0.021$, where $\delta(\Delta E)_{\text{std}}$ is as computed by Babushkin[43] but is corrected by 5.6% for the interaction of the electron's anomalous moment with the nuclear field.[44] The anomalous moment shift opposes the volume IS and should, for consistency, be applied to the optical C_{std} as well. Using Babushkin's[45] values for C_{std} and including the anomalous moment correction, we find

TABLE IV. Skin thickness variations in Sn.

Isotope pair	$\frac{\delta(R_u)_t}{\delta(R_u)_{\text{std}}}$(muonic)	$\frac{\delta(R_u)_{\text{expt}}}{\delta(R_u)_{\text{std}}}$(electronic)	$\delta t/t$ (%)
116–118	0.630±0.023	0.585±0.03	−1.4±0.4
118–120	0.521±0.014	0.609±0.03	2.5±0.3
120–122	0.508±0.016	0.525±0.03	0.5±0.3
117–120	0.620±0.010	0.614±0.08	−0.3±1.2
119–120	0.768±0.040	1.11 ±0.21	5.0±3.3

that the muonic data are best fit for m (3283 Å)$=(3.3\pm 0.6)\times 10^{-3}$ cm^{-1}/neutron, while the electronic x-ray result implies $m=(3.0\pm 0.4)\times 10^{-3}$ cm^{-1}. We have allowed for the effect upon m of a $\pm 5\%$ uncertainty in the electronic factor F.

Since the electronic and muonic x-ray IS appear to be consistent, we construct a second Brix-Kopfermann plot with $m=3.0\times 10^{-3}$ cm^{-1} (Fig. 6, full line). This plot shows much better accord between the muonic and the electronic estimates for $\delta(R_u)_t/\delta(R_u)_{\text{std}}$.

Notwithstanding the gratifying qualitative agreement between the muonic and the revised optical IS, several quantitative discrepancies are evident in Fig. 6, particularly the one for Sn^{118}–Sn^{120}. Recalling that the muonic $\delta(R_u)$ are inherently model-dependent, it is of interest to estimate the isotopic changes in skin thickness which would be required to produce exact agreement (Table IV). For the even Sn isotopes, the required change in t never exceeds 3% of its mean value; even for Sn^{119}–Sn^{120}, the least accurately known shift, only a 5% adjustment in t need be made. Thus the deduced changes in skin thickness are of "reasonable" magnitude.

One might perhaps attempt to relate these changes in t to changes in $\langle\beta^2\rangle$, the mean-squared deformation. For the Sn isotopes, where $\langle\beta^2\rangle\approx 0.1$,[4] we expect, quite roughly, $\delta t\cong 35\delta\langle\beta^2\rangle F$. Uncertainties in the values of $\langle\beta^2\rangle$ derived from Coulomb excitation experiments[46] are unfortunately of just the same magnitude as the changes in $\langle\beta^2\rangle$ suggested by the muonic IS.

We conclude that there is no real disagreement between the muonic and electronic IS for Sn. The optical results agree with the x-ray data (both electronic and muonic) if the specific mass shift in the 3283-Å line is taken as $m=(3.0\pm 0.4)\times 10^{-3}$ cm^{-1}/neutron [as opposed to Stacey's original estimate of $(4\pm 3)\times 10^{-3}$ cm]. The revised atomic and the muonic measurements can be brought into exact agreement by allowing in the muonic shifts for slight isotopic changes in skin thickness.

The recent electron scattering work[47] of Barreau and Bellicard on Sn^{116}, Sn^{120}, and Sn^{124} is not sufficiently precise to usefully predict muonic IS but suggests that Sn^{120} has a larger skin thickness than does Sn^{116}, in agreement with our analysis.

[41] W. R. Hindmarsh and H. Kuhn, Proc. Roy. Soc. (London) **A68**, 443 (1966).
[42] D. N. Stacey (private communication).
[43] F. A. Babushkin, Opt. i Spektroskopiya **15**, 721 (1963) [English transl.: Opt. Spectry. (USSR) **15**, 393 (1963)].
[44] G. Breit and W. W. Clendenin, Phys. Rev. **85**, 689 (1952).
[45] F. A. Babushkin, Zh. Eksperim. i Teor. Fiz. **45**, 1478 (1963) [English transl: Soviet Phys.—JETP **18**, 1022 (1963)].
[46] P. H. Stelson and F. K. McGowan, Phys. Rev. **110**, 489 (1958).
[47] P. Barreau and J. B. Bellicard, Phys. Letters **24B**, 470 (1967).

TABLE V. Sr and Zr isotope shifts.

Isotope pair	Observed shift (keV)	Volume shift (keV)	$\frac{\delta(R_u)_t}{\delta(R_u)_{std}}$(muonic)	$\frac{\delta(R_u)_t}{\delta(R_u)_{std}}$(optical)
Sr				
84–86	...	...	...	$-0.3 \rightarrow +0.2$
86–88	-1.35 ± 0.12	-1.27 ± 0.12	-0.192 ± 0.018	$-0.2 \rightarrow +0.2$
88–90	...	...	...	$+1.1 \rightarrow +1.6$
86–87	-1.15 ± 0.10	-1.11 ± 0.10	-0.177 ± 0.016	...
Zr				
90–92	8.2 ± 0.4	8.3 ± 0.4	1.14 ± 0.06	$1.10+0.12$
92–94	...	...	...	$0.78+0.12$
94–96	...	...	...	0.61 ± 0.13

A. Strontium and Zirconium

For these elements, it is not possible to make detailed comparison with the optical data. In the case of Sr, these data[48,49] merely show that the shifts are very likely much smaller than the $A^{1/3}$ expectations. For Zr, we measure only one shift and thus can check only roughly the specific mass shift estimates of Heilig *et al.*[50]

1. Strontium

The optical IS in the isotopes Sr^{84}, Sr^{86}, and Sr^{88} were first measured by Hughes.[48] He found no significant difference between the 84–86 and 86–88 shifts, and concluded that, for both pairs, the volume shifts were consistent with zero. Heilig[49] repeated Hughes's measurements with greater precision and, in addition, measured the Sr^{88}–Sr^{90} isotope shift. He refined Hughes's conclusions somewhat, setting reasonable limits on the specific mass contributions to the Sr I and Sr II shifts by surveying the mass shifts in the analogous transitions of lighter elements. Using values of C_{std} calculated by Humbach,[51] he arrived at the estimates of $\beta C_{expt}/C_{std}$ $[\equiv \delta(R_u)_t/\delta(R_u)_{std}]$ given in Table V. Regardless of the sizeable uncertainties due to inadequate knowledge of the specific mass shifts, it is apparent that the Sr^{84}–Sr^{86} and Sr^{86}–Sr^{88} shifts are much smaller in magnitude than is the Sr^{88}–Sr^{90} shift. This large change in volume shift upon closure of the neutron shell at $N=50$ is very reminiscent of the shifts observed in Ce near $N=82$.[52,53] The optical results are compared with our muonic data in the same table. The agreement is quite satisfactory and indicates that both Sr^{87} and Sr^{88} are "more compact" than Sr^{86}, thus reinforcing our belief in the strong influence of shell structure on IS. It is suggested that the specific mass effect in Sr II is small and opposite in sign to the normal mass effect.

TABLE VI. Other isotope shifts.

Isotope pair	Observed shift (keV)	Volume shift (keV)	$\delta(R_u)_t/\delta(R_u)_{std}$
Si^{28}–Si^{29}	-0.08 ± 0.04	-0.03 ± 0.04	-0.07 ± 0.09
Si^{28}–Si^{30}	0.00 ± 0.04	$+0.10\pm0.04$	$+0.12\pm0.05$
K^{39}–K^{41}	0.35 ± 0.06	0.45 ± 0.06	0.31 ± 0.04
Fe^{54}–Fe^{5}	2.97 ± 0.12	3.06 ± 0.14	0.94 ± 0.05
Fe^{56}–Fe^{57}	1.25 ± 0.20	1.29 ± 0.20	0.81 ± 0.12
Ni^{58}–Ni^{60}	3.14 ± 0.14	3.23 ± 0.14	0.83 ± 0.04
Ni^{60}–Ni^{61}	0.97 ± 0.18	1.01 ± 0.18	0.53 ± 0.09
Ni^{60}–Ni^{62}	2.00 ± 0.17	2.09 ± 0.17	0.55 ± 0.04
Cu^{63}–Cu^{55}	2.31 ± 0.16	2.40 ± 0.16	0.60 ± 0.04

2. Zirconium

Heilig *et al.*[50] measured optical IS in Zr^{90}, Zr^{92}, and Zr^{94}. They were able (by analogy with transitions in lighter elements) to estimate the specific mass shift as less than one-half of the normal mass shift, and hence to extract the volume shifts with fair ($\sim 20\%$) accuracy. There is again apparent an especially large shift (Zr^{90}–Zr^{92}) after shell closure at $N=50$. The muonic result, also given in Table V, agrees very well with the optical work.

VII. OTHER NUCLIDES

Apart from the elements already discussed, this experiment measured x-ray shifts in isotopes of Si, K, Fe, Ni, and Cu. In no case do there exist either theoretical predictions or other experimental results for these elements. We shall be content therefore to merely state the results (see Table VI), pointing out the more interesting features.

A. Silicon and Potassium

The very small IS seen here may perhaps reflect the incomplete saturation of nuclear forces below $A \sim 60$. In the case of Si, believed to be strongly deformed, changes in R_u may also be largely due to changes in deformation.

B. Iron, Nickel, and Copper

Perhaps the most interesting effect observed here is the large Fe^{54}–Fe^{56} IS again occurring after closure of a major neutron shell, and demonstrating the "magicness" of $N=28$ in a manner complementary to the Ca^{40}–Ca^{48}

[48] R. H. Hughes, Phys. Rev. **105**, 1260 (1957).
[49] K. Heilig, Z. Physik **161**, 252 (1961).
[50] K. Heilig, K. Schmitz, and A. Steudel, Z. Physik **176**, 120 (1963).
[51] W. Humbach, Z. Physik **133**, 589 (1952).
[52] H. Arroe, Phys. Rev. **93**, 94 (1954).
[53] P. Brix and H. Frank, Z. Physik **127**, 289 (1950).

TABLE VII. Absolute $K\alpha$ energies (keV).

Nuclide	This experiment $K\alpha$ (center of gravity)	This experiment $K\alpha_1$	This experiment $\Delta 2p$	Other determinations $K\alpha$ (center of gravity)	Other determinations $K\alpha_1$	Other determinations $\Delta 2p$
Si (nat)	400.2 ±0.6			400.15±0.15[a]		
				400.22±0.15[b]		
K (nat)	712.64±0.23			714.1 ±4[c]		
Ca (nat)	783.56±0.16			783.85±0.15[b]		
				783.8 ±1.5[d]		
				780.8 ±0.8[e]		
Fe (nat)	1254.9 ±0.3			1256.4 ±2.4[d]		
				1255.5 ±2.4[f]		
				1254.5 ±4.0[e]		
Ni^{60}	1427.6 ±0.6					
Ni (nat)	1429.5 ±0.6			1428.5 ±5[c]		
				1427.4 ±2[g]		
Cu^{63}	1511.0 ±0.6					
Cu (nat)	1510.3 ±0.6			1507.3 ±4.4[f]		
				1511.4 ±1.0[e]		
				1515.1 ±6[c]		
				1510.7 ±2[g]		
Sr (nat)	2235.6 ±0.8	2241.5±0.4	17.5			
Zr^{90}	2528.9 ±0.8	2535.9±0.4	21.0	2534.0 ±5.1[h]		
Sn^{120}	3439.2 ±1.0	3454.5±0.5	45.8±0.2			
Sn (nat)	3442.4 ±1.0	3457.7±0.5	45.8±0.2	3446.4 ±6.4[h]		
				(3441.6 ±3.5	3457.3±3.0	44.5±1.5)[d]

[a] G. Backenstoss, S. Charalambus, H. Daniel, H. Koch, G. Poelz, H. Schmidt, and L. Tauscher, Phys. Letters **25B**, 547 (1967).
[b] Reference 39.
[c] D. Quitmann, R. Engfer, U. Hegel, P. Brix, G. Backenstoss, K. Goebel, and B. Stadler, Nucl .Phys. **51**, 609 (1964).
[d] Reference 38.
[e] J. A. Bjorkland, S. Raboy, C. C. Trail, R. D. Ehrlich, and R. J. Powers, Nucl. Phys. **69**, 161 (1965).
[f] W. Frati and J. Rainwater, Phys. Rev. **128**, 2360 (1962).
[g] S. Devons, in Proceedings of the Williamsburg Conference on Intermediate Energy Physics (unpublished).
[h] H. L. Anderson, C. S. Johnson, and E. P. Hincks, Phys. Rev. **130**, 2468 (1963).

shift. This closed-shell phenomenon has now been seen for $N=28$, 50 and 82. It appears to point out magic numbers in much the same way as do cusps in mass-defect plots. Though there is no stable Ni isotope with $N=28$, the Ni^{58}–Ni^{60} shift, still rather large compared to the Ni^{60}–Ni^{62} shift, may reflect the proximity of Ni^{58} to a closed shell.

VIII. K-Ca ISOTONE SHIFTS

It is well known that nuclear charge radii along the valley of maximum stability follow an $A^{1/3}$ dependence fairly well, at least for $A \gtrsim 20$.[35] It is apparent from the IS data, however, that addition of neutrons to a nucleus produces too small an expansion to be consistent with an $A^{1/3}$ law. One expects, therefore, that the average $\delta(R_u)$ produced by addition of a proton to a nucleus ought to exceed the $A^{1/3}$ expectation. Earlier muonic experiments[54] have surveyed a variety of isotone shifts and have found this to be generally the case. The bulk of the observed x-ray shift between isotones is, of course, purely due to Coulomb effects; thus, it is difficult to achieve here the accuracy possible for IS.

It was a fringe benefit of the four-target scheme employed in this experiment that we could accumulate data on the Ca^{40}–Ca^{42} and K^{39}–K^{41} IS concurrently. The same approach used to analyze the IS was applied to the K^{39}–Ca^{40} and K^{41}–Ca^{42} isotone shifts. The energy differences involved here are ≈ 70 keV, as opposed to the isotopic differences which are typically ≈ 0.5 keV. It was found, however, that the same master line shape gave excellent fits to both the K and Ca data. The error assigned has nevertheless been doubled to allow for possible systematic differences in line shape. The observed $K\alpha$ energy differences for K^{39}–Ca^{40} and K^{41} and Ca^{42} are, respectively, (70.92±0.15) keV and (70.59±0.15) keV. These numbers refer to the separation between the centers of gravity of the fine-structure patterns and have been corrected for minor isotopic impurities. If we again assume $\delta t \equiv 0$, and choose reasonable values for the charge radii of Ca^{40}–Ca^{42}, we find that an $A^{1/3}$ law would imply corresponding predictions of 71.32 and 71.07 keV. Adjustment of the K^{39} and K^{41} charge radii so as to give agreement with the data yields the results

$$\delta(R_u)_t/\delta(R_u)_{\text{std}} = 1.40 \pm 0.20, \quad K^{39}\text{–}Ca^{40}$$

TABLE VIII. Calibration γ-ray energies.

Source	γ-ray energy (keV)
Na^{24}	511.006±0.002[a]
Cs^{137}	661.595±0.08[a]
Mn^{54}	834.80 ±0.07[b]
Co^{60}	1173.226±0.04[a]
Co^{60}	1332.48 ±0.05[a]
Na^{24}	1368.53 ±0.04[a]
Na^{24}	1731.91 ±0.12[a] (2-quantum escape)
Na^{24}	2753.92 ±0.12[a] (full energy)

[a] G. Murray, R. L. Graham, and J. S. Geiger, Nucl. Phys. **63**, 353 (1965).
[b] A. V. Ramayya, J. H. Hamilton, S. Brahmavar, and J. J. Pinajian, Phys. Rev. Letters **24B**, 49 (1967).

[54] D. Quitmann, Z. Physik **206**, 113 (1967).

and

$$\delta(R_u)_t/\delta(R_u)_{\text{std}}=1.64\pm0.20, \quad K^{41}\text{–}Ca^{42}.$$

The large isotone shift persists in spite of the closed proton shell in Ca.

IX. ABSOLUTE $K\alpha$ X-RAY ENERGIES

While the present experiment was designed primarily to measure isotope shifts, the excellent stability and linearity of the linear system enabled us to measure absolute energies to high accuracy. Table VII summarizes the results, corrected for isotopic impurities via the measured isotope shifts. We present also the derived x-ray energies for the naturally occurring isotopic mixtures for convenience in comparing with other work. The $2p_{3/2}$-$2p_{1/2}$ fine structure has been assumed known, except in the case of Sn^{120}, where it has been measured to be (45.83±0.20) keV. The present results are nowhere in disagreement with earlier measurements, but are generally quoted to considerably improved accuracy. Table VIII lists the calibration energies used in the analysis.

X. SUMMARY: CONCLUDING REMARKS

We have demonstrated the degree to which accurately measured muonic IS can provide information about changes in nuclear size. The IS have been extended to previously unexplored regions of the periodic table; they show in all cases large departures from an $A^{1/3}$ behavior. Particularly striking are apparent shell-closure effects in Ca, Fe, Sr, and Zr. In those cases where the muonic data can be compared with other measurements, we find the corresponding IS in good agreement, provided allowance is made for model dependence of the muonic $\delta(R_u)$ in comparing with the IS in electronic atoms.

It is unfortunate that there is at present no theory for the IS with predictive power commensurate with the accuracy attained in this experiment. A rough (~20%) estimate of the Ca^{40}–Ca^{44} IS by Mikulinskiĭ and Osadchiev,[55] based on the Midgal theory of finite Fermi systems, differs significantly from our result (2.1 keV predicted versus 0.89 keV observed).

Perhaps the most satisfying predictions for the IS might emerge from a very ambitious program of self-consistent field calculations after the manner of Brueckner *et al.*[56] To date, however, the IS data (from electron scattering) has generally been approached from a different aspect. Together with other experimental quantities (proton separation energies, nuclear masses, etc.), the IS data are used as input information in various phenomenological shell-model calculations.[57–59] The derived quantities are the parameters describing the (single-particle) shell-model potential well. The manner in which these parameters vary with atomic mass gives *a posteriori* understanding of the IS and also tests the validity of the nuclear model. While the calculations differ in their details, all provide proton distributions which fit the electron scattering data for Ca remarkably well. The neutron wave functions are also available and may be compared with experimental results on the Coulomb displacement energies of isobaric analog pairs.[60]

Considering the very rapid advance of technology in muonic x-ray, electron scattering, and electronic x-ray work, it seems likely that a very large collection of precise IS results will soon become available to challenge and perhaps inspire the nuclear theorist.

ACKNOWLEDGMENTS

It is difficult to find words to properly thank the many individuals whose efforts made this work possible. Professor V. L. Telegdi, who suggested the IS experiment, has my sincere thanks for guidance, excellent ideas, and cogent criticism throughout the experiment as well as during the writing of this paper. To Professor H. L. Anderson who arranged for the sharing of the apparatus and to C. K. Hargrove, without whose efforts the experiment could not have succeeded, I am particularly indebted. Likewise, I thank my other collaborators, D. Fryberger, D. Jensen, C. Nissim-Sabat, and R. J. Powers for their invaluable contributions (including many weeks of hard work) to the performance of the experiment. I am grateful to Frank Castorf and Mrs. Serena Torres, whose programming talents kept the two computers under firm control, and to R. J. McKee who wrote the program to calculate the muonic energy levels. To D. White and Dr. K. Haefner are due thanks for their extensive assistance in preparing the isotopic targets. I am indebted to Dr. G. Rogosa (AEC) for his help in procuring the separated isotopes, to Professor E. Shrader and Professor H. Newson for graciously lending us isotopes which they obtained for their own use only with difficulty, and to Dr. D. N. Stacey (Oxford) and Professor D. G. Ravenshall and Professor F. Boehm for helpful correspondence. Finally, I thank Mrs. Elizabeth Bitoy for typing the manuscript, and my wife for her understanding and encouragement.

[55] M. A. Mikulinskiĭ and V. M. Osadchiev, Yadern. Fiz. **3**, 639 (1966) [English transl.: Soviet J. Nucl. Phys. **3**, 467 (1966)].
[56] K. A. Brueckner, A. M. Lockett, and M. Rotenberg, Phys. Rev. **121**, 255 (1961).
[57] A. Swift and L. R. B. Elton, Phys. Rev. Letters **17**, 484 (1966).
[58] L. R. B. Elton and A. Swift, Nucl. Phys. **A94**, 52 (1967).
[59] B. F. Gibson and K. J. van Oostrum, Nucl. Phys. **A90**, 159 (1967).
[60] J. A. Nolen, Jr., J. P. Schiffer, N. Williams, and D. von Ehrenstein, Phys. Rev. Letters **18**, 1140 (1967).